San Jose State University

SJSU ScholarWorks

1-1-2008

Microfluidic devices for terahertz spectroscopy of biomolecules

P. A. George
Cornell University

W. Hui
Cornell University

F. Rana
Cornell University

Benjamin G. Hawkins
San Jose State University, bghawkin@calpoly.edu

A. E. Smith
Cornell University

See next page for additional authors

Recommended Citation

Authors

P. A. George, W. Hui, F. Rana, Benjamin G. Hawkins, A. E. Smith, and B. J. Kirby

Microfluidic devices for terahertz spectroscopy of biomolecules

Paul A. George[1]**, Wallace Hui**[1]**, Farhan Rana**[1]**, Benjamin G. Hawkins**[2]**,
A. Ezekiel Smith**[3]**, Brian J. Kirby**[4]

[1]*School of Electrical and Computer Engineering, Cornell University, Ithaca, NY, 14853*
[2]*Department of Biomedical Engineering, Cornell University, Ithaca, NY, 14853*
[3]*School of Applied and Engineering Physics, Cornell University, Ithaca, NY, 14853*
[4]*School of Mechanical and Aerospace Engineering, Cornell University, Ithaca, NY, 14853*

pag25@cornell.edu

Abstract: We demonstrate microfluidic devices for terahertz spectroscopy of biomolecules in aqueous solutions. The devices are fabricated out of a plastic material that is both mechanically rigid and optically transparent with near-zero dispersion in the terahertz frequency range. Using a low-power terahertz time-domain spectrometer, we experimentally measure the absorption spectra of the vibrational modes of bovine serum albumin from 0.5 - 2.5 THz and find good agreement with previously reported data obtained using large-volume solutions and a high-power free-electron laser. Our results demonstrate the feasibility of performing high sensitivity terahertz spectroscopy of biomolecules in aqueous solutions with detectable molecular quantities as small as 10 picomoles using microfluidic devices.

OCIS codes: (300.0300) Spectroscopy; (280.0280) Remote sensing and sensors; (230.0230) Optical devices; (17.0170) Medical optics and biotechnology

References and links

1. S. Hayward and N. Go, "Collective variable description of native protein dynamics," Annu. Rev. Phys. Chem. **46,** 223–250 (1995).
2. M.C. Chen and R.C. Lord, "Laser-excited Raman spectroscopy of biomolecules: conformational study of bovine serum albumin," J. Am. Chem. Soc. **98,** 990–992 (1976).
3. W. Zhuang, Y. Feng, and E.W. Prohofsky, "Self-consistent calculation of localized DNA vibrational properties at a double-helix–single-strand junction with anharmonic potential," Phys. Rev. A **41,** 7033–7042 (1990).
4. A.G. Markelz, and A. Roitberg, and E.J. Heilweil, "Pulsed terahertz spectroscopy of DNA, bovine serum albumin and collagen between 0.1 and 2.0 THz," Chem. Phys. Lett. **320**, 42–48 (2000).
5. T.R. Globus, D.L. Woolard, T. Khromova, T.W. Crowe, M. Bykhovskaia, B.L. Gelmont, J. Hesler, and A.C. Samuels, "THz-spectroscopy of biological molecules," J. Bio. Phys. **29**, 89–100 (2003).
6. T.R. Globus, D.L. Woolard, T.W. Crowe, T. Khromova, M. Bykhovskaia, B.L. Gelmont, and J. Hesler, "Terahertz Fourier transform characterization of biological materials in a liquid phase," J. Phys. D **39**, 3405–3413 (2006).
7. J. Xu, K.W. Plaxco, and S.J. Allen, "Probing the collective vibrational dynamics of a protein in liquid water by terahertz absorption spectroscopy," Prot. Sci. **15**, 1175–1181 (2006).
8. M. Nagai, H. Yada, T. Arikawa, and K. Tanaka, "Terahertz time-domain attenuated total reflection spectroscopy in water and biological solutions," Intl. J. Inf. and Mill. Waves **27**, 505–515 (2006).
9. J. Kitagawa, T. Ohkubo, M. Onuma, and Y. Kadoya, "THz spectroscopic characterization of biomolecule/water systems by compact sensor chips," Appl. Phys. Lett. **89**, 041114 (2006).
10. T. Baras, T. Kleine-Ostmann, and M. Koch, "On-chip THz detection of biomaterials: a numerical study," J. Bio. Phys. **29**, 187–194 (2003).
11. M. Nagel, P.H. Bolivar, M. Brucherseifer, H. Kurz, A. Bosserhoff, and R. Büttner, "Integrated THz technology for label-free genetic diagnostics," Appl. Phys. Lett. **80**, 154 (2002).
12. "Zeonor Production Information Sheet," Zeon Corporation (2004).

13. T.I. Wallow, A.M. Morales, B.A. Simmons, M.C. Hunter, K.L. Krafcik, L.A. Domeier, S.M. Sickafoose, K.D. Patel, and A. Gardea, "Low-distortion, high-strength bonding of thermoplastic microfluidic devices employing case-II diffusion-mediated permeant activation," Lab on a Chip **7**, 1825–1831 (2007).
14. B.G. Hawkins, A.E. Smith, Y.A. Syed, and B.J. Kirby, "Continuous-flow particle separation by 3D insulative dielectrophoresis using coherently shaped, dc-biased, ac electric fields," Anal. Chem. **79**, 7291-7300(2007).
15. "Bovine Serum Albumin Product Information Sheet," Sigma-Aldrich (2000).
16. R.D. Levine, *Molecular Reaction Dynamics*, Cambridge Univeristy Press (2005).

1. Introduction

Important biomolecules, including proteins, RNA, and DNA have vibrational modes with frequencies in the 0.1 THz - 5 THz range [1, 2, 3, 4, 5, 6, 7, 9, 10, 11]. These modes correspond to collective molecular oscillations and rotations as well as the relative motion of molecular subdomains [1, 2, 3].

Several studies of biomolecules in the THz frequency range have been conducted [4, 5, 6, 7, 8, 9, 10, 11]. Due to strong water absorption at THz frequencies, these studies have typically been limited to dry or partially hydrated specimens. In [4], THz time-domain spectroscopy (THz-TDS) was performed on dried films of biomolecules that were up to 7.5 mm thick. In [5, 6], THz-TDS of hydrated liquid-phase biomolecules prepared in gel films was performed. Studies of the THz absorption of biomolecules in large volume aqueous solutions were conducted in [7], but these experiments required the use of a high-power free electron laser. Unfortunately, such high-power THz sources are not readily available. THz-TDS of smaller volumes of sucrose solutions was demonstrated using attenuated total reflection spectroscopy [8]. Recently, integrated spectroscopy systems based upon microstrip waveguides have been proposed and demonstrated in [9, 10, 11]. The performance of these devices suffers from the limited bandwidth of microstrip components.

In this paper, we demonstrate microfluidic channels for THz spectroscopy of biomolecules. Performing spectroscopy of biomolecules in microfluidic devices can be advantageous for the following reasons: (1) biological specimens can be interchanged or reacted in real-time; (2) the dimensions of microfluidic channels can be designed to facilitate the use of low-power THz-TDS systems by avoiding excess water absorption and to enable the spectroscopy of picomole quantities of biomolecules; and, (3) microfluidic channels can easily be integrated with photonic components to realize multifunctional spectroscopy platforms. A schematic of a THz sensing platform based on microfluidic channels is shown in Fig. 1. The realization of such devices requires materials that have low loss and dispersion from optical to THz frequencies, are mechanically stable and chemically inert, and are compatible with microfabrication.

Using microfluidic devices, we measure the absorption coefficient of the protein bovine serum albumin (BSA) in the 0.5 THz - 2.5 THz frequency range with a detection sensitivity approaching 1.5 micromole/mL. The measured spectrum is in excellent quantitative agreement with the previously reported results in [7]. Our results demonstrate the feasibility of performing THz spectroscopy of picomole quantities of biomolecules in microfluidic devices using sub-microWatt low-power THz sources.

2. Microfluidic devices for THz spectroscopy

Microfluidic channels are commonly fabricated from polydimethylsiloxane elastomer (PDMS), which has high water content and therefore exhibits large absorption at THz frequencies. The microfluidic devices used in this work were fabricated from Zeonor 1020R (Zeon Corporation), a cyclo-olefin polymer that has high transmission from UV to Far-IR wavelengths, is mechanically robust, and has significantly lower water content than PDMS [12].

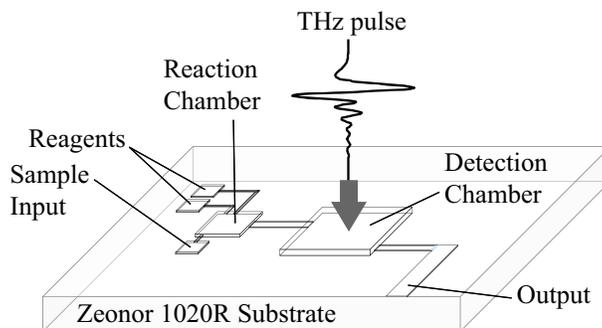Terahertz time-domain scans of a 2 mm slab of Zeonor 1020R and a 1 mm slab of PDMS

Fig. 1. A system for on-chip THz sensing. The device contains sample and reagent inputs, a reaction chamber, and a detection chamber for THz as well as optical and IR spectroscopy.

were conducted using a THz-TDS based on a $<100>$ n-InAs (5×10^{16} cm^{-3}) emitter and a 1 mm $<110>$ ZnTe electro-optic detector. The emitter was pumped by 1 W of optical power from a 90 fs Ti:Sapphire ultrafast laser (780 nm) with an 86 MHz repetition rate. The THz pulses had a bandwidth of 0.25 THz - 3 THz and the THz-TDS had a power SNR approaching 10^6. To eliminate absorption from water vapor, the entire experimental setup was encased in a nitrogen-purged plastic box. The measured error in the repeatability of successive scans was less than 5% and is attributable to the drift of optomechanical components and the laser beam.

Because both the Zeonor and PDMS slabs were thick and exhibited only broad spectral features, we limited the spectrometer scan length so as to avoid etalon effects caused by multiple internal reflections. The index of refraction and absorption coefficient of Zeonor and PDMS were extracted using Fresnel's equation for the frequency-dependent amplitude transmission through a dielectric slab, t, without multiple internal reflections

$$t = \frac{E_m(\omega)}{E_r(\omega)} = \frac{4n}{(1+n)^2} e^{i\frac{\omega}{c}(n-1)d} \tag{1}$$

In Eq. 1, $E_m(\omega)$ is the measured THz spectrum of the pulse after propagation through the slab, $E_r(\omega)$ is the THz spectrum of the reference pulse, d is the slab thickness, and n is the complex index of refraction of the slab. The absorption coefficients of Zeonor and PDMS calculated from the extracted complex indices of refraction are shown in Fig. 2.

Zeonor 1020R has a measured index of approximately 1.518 and an absorption coefficient <1 cm^{-1} from 0.5 THz - 2.5 THz. The low absorption of Zeonor over a large frequency range makes it better suited for terahertz spectroscopy than PDMS.

Fabrication of microfluidic devices out of Zeonor 1020R has previously been described in [13, 14] and is shown pictorially in Fig. 3(a) and (b). The Si template for embossing the fluidic channel in Zeonor was constructed using standard photolithography techniques and deep Si etching. The final device was 5 mm wide, 25 mm long, and 95 μm deep. A 14.5 cm^2 square Zeonor piece was embossed with the template on a hotpress at a temperature of 115 C and a pressure of 2.55 MPa. The piece was then cooled under load until its temperature was below the glass transition temperature (102 C [12]). Fluid input and output ports were then defined. Next, the embossed piece and a blank 14.5 cm^2 Zeonor square were soaked in an ethanol/decalin (80/20) solution for 30 s and 1 min, respectively. The pieces were then rinsed in ethanol, dried and bonded on a hotpress at a temperature of 65 C and a pressure of 1.6 MPa for 40 min to form the channel. A picture of a typical completed device is shown in Fig. 3(b).
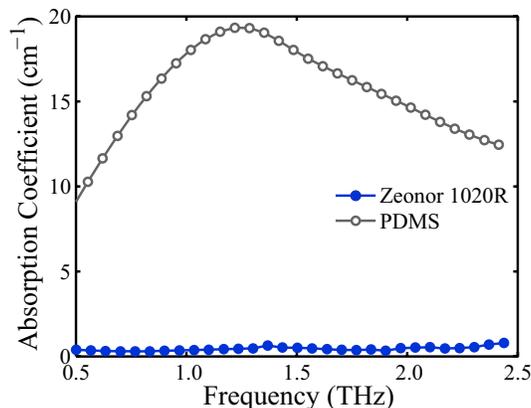
Fig. 2. The measured absorption coefficient of Zeonor 1020R and PDMS. Zeonor has a nearly constant index of 1.518 (not shown) and an absorption coefficient <1 cm^{-1} at THz frequencies, which is 10-20 times smaller than that of PDMS.
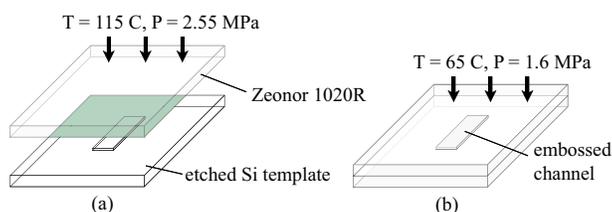

Fig. 3. Fabrication of the microfluidic devices used in this work. (a) A slab of Zeonor 1020R was first embossed using a Si template. (b) The embossed slab was then bonded to another piece of Zeonor 1020R. The final channel depth was 95 μm.

3. Measurement of the THz absoprtion spectrum of BSA in microfluidic channels

As a proof of principle, we measured the absorption spectrum of the protein bovine serum albumin (BSA) in Zeonor microfluidic channels. BSA is a well studied proteins and has previously been used in the study of biomolecules at THz frequencies [4, 7, 9]. It is a polypeptide chain consisting of 583 amino acids [15] with a sequence homology similar to Human Serum Albumin [7]. It has an ellipsoidal geometry [2] with a 54% α-helix and 18% β-sheet structure and has a molecular weight of approximately 66.430 kDa [15].

Aqueous solutions of globulin-free and fatty-acid-free lyophilized BSA powder (Sigma-Aldrich A0281 Batch #075K7545) were prepared in a 0.05 M phosphate buffer (pH = 7.5) at concentrations of 101 mg/mL (pH = 7.0), 200 mg/mL (pH = 6.9), and 305 mg/mL (pH = 6.9) as measured by 279 nm UV spectrophotometry. At these high concentrations, the uncertainty in the measurement of the BSA concentration was approximately $\pm10\%$.

The complex THz transmission spectra of the empty microfluidic channel, the channel filled with phosphate buffer, and the same channel filled with the BSA solutions were obtained in succession. To avoid perturbing the experimental setup, the solutions were pumped into the channel with syringes connected to long Tygon tubing. Scans of the phosphate buffer with a 0.02 THz resolution and BSA solutions exhibited no significant features with spectral width less than 0.15 THz between 0.5 THz - 2.5 THz. This observation is consistent with the THz absorption spectra of water and BSA reported in [4, 7, 9].

The THz transmission of each solution was averaged over three successive scans with a

measured reproducibility near 98%. Equation 1 is not valid for extracting the absorption coefficient from the measured THz transmission because multiple internal reflections inside the 95 μm channel cannot be ignored. Instead, we have used Eq. 2 which includes these effects but neglects multiple reflections from the thick Zeonor slabs on either side of the channel.

$$t = \frac{E_s(\omega)}{E_a(\omega)} = n_s e^{i\frac{\omega}{c}(n_s-1)d_c} \left[\frac{(n_z+1)^2 - (n_z-1)^2 e^{2i\frac{\omega}{c}d_c}}{(n_z+n_s)^2 - (n_z-n_s)^2 e^{2i\frac{\omega}{c}n_s d_c}} \right] \qquad (2)$$

$E_s(\omega)$ and $E_a(\omega)$ are the measured THz spectra of the pulse after propagation through the channel filled with solution and with air, respectively. d_c is the channel depth, n_z and n_s are the complex indices of Zeonor and the solution, respectively.

The extracted absorption coefficients of the phosphate buffer and BSA solutions are shown in Fig. 4. Consistent with the experimental results in [9], a monotonic decrease in the absorption coefficient of the BSA solution with increasing concentration is observed. This is due to the expulsion of solvent molecules by less-absorbing BSA molecules. The change in absorption coefficient between the 0.05 M phosphate buffer and the 101 mg/mL BSA solution is 15 cm^{-1} - 20 cm^{-1}, or 8%.
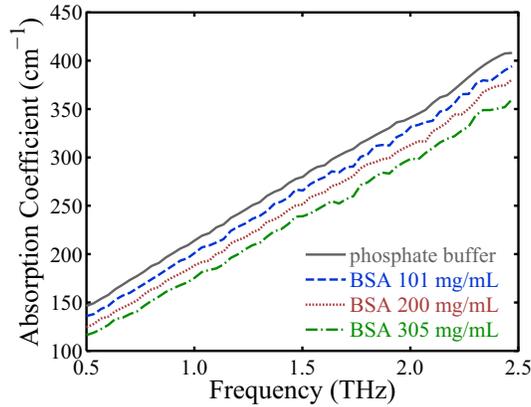

Fig. 4. The absorption coefficient of the phosphate buffer and BSA solutions measured by THz-TDS using microfluidic devices. Values are extracted using Eq. 2.

The total THz absorption coefficient of the BSA solution, α_s, can be written as,

$$\alpha_s = \alpha_{bsa} \frac{V_{bsa}}{V_{bsa} + V_{pb}} + \alpha_{pb} \frac{V_{pb}}{V_{bsa} + V_{pb}} \qquad (3)$$

where α_{bsa} and α_{pb} are the absorption coefficients of the hydrated BSA molecules and the phosphate buffer (Fig. 4), respectively. V_{bsa} and V_{pb} are the volumes of the BSA and phosphate buffer in the solution. Based upon density measurements of BSA solutions reported in [7], a molecular radius of 2.8 nm for hydrated BSA was used to calculate V_{bsa}. Figure 5(a) displays the extracted values of α_{bsa} as a function of frequency. The error bars indicate the observed $\pm 10\%$ error in the measurement of the concentrations of the BSA solutions. Oscillations in the data for the 101 mg/mL solution near 2 THz are attributable to low SNR and are not present at higher concentrations. The absorption coefficient plotted in Fig. 5(a) approaches zero at low frequencies and increases nearly monotonically from 0.5 THz - 2.5 THz due to the increase in the density of molecular vibrational modes [7]. The values of the absorption coefficient extracted from measurements of the 101 mg/mL and 200 mg/mL BSA solutions do not exhibit significant concentration dependence in agreement with Beer's Law [16]. The slight reduction in the

extracted absorption coefficient for the 305 mg/mL solution is most likely due to uncertainties in the measured solution concentration.

The molar extinction of BSA molecules in aqueous solution (cm^{-1} M^{-1}), α_{mbsa}, is related to α_{bsa} by

$$\alpha_{mbsa} = \alpha_{bsa} N_A V_{mbsa} \qquad (4)$$

where N_A is Avogadro's Number and V_{mbsa} is the volume of a hydrated BSA molecule in liters [7]. In Fig. 5(b), we compare our measurement of the molecular extinction of BSA to those reported in [7] using large-volume aqueous solutions of BSA and a high-power THz free-electron laser. The good agreement from 0.5 - 2.5 THz demonstrates the feasibility of performing THz spectroscopy of biomolecules in aqueous solutions using microfluidic channels using low-power THz sources. It should be noted no scaling was used to achieve the fit Fig. 5(b) and that the data is absolute, within the indicated error margins.
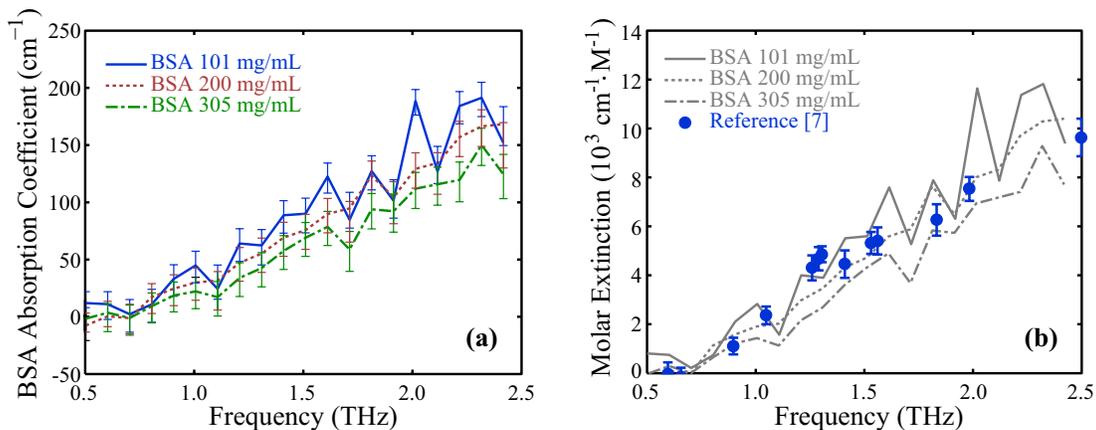

Fig. 5. (a) The measured molecular absorption coefficient of hydrated BSA molecules. In agreement with Beer's Law, the absorption coefficient does not depend on solution concentration. (b) The molar extinction of BSA measured using microfluidic channels compared to the results in [7]. The excellent agreement demonstrates the feasibility of performing THz spectroscopy of biomolecules in microfluidic channels using low-power THz sources.

4. Conclusion

We have demonstrated for the first time terahertz time-domain spectroscopy of bovine serum albumin in aqueous solution using Zeonor microfluidic channels. The measured results agree well with those previously reported using high-power THZ free-electron lasers [7]. Assuming a minimum BSA solution concentration of 100 mg/mL, a microfluidic channel of area 500×500 μm^2, and a channel depth of 50 μm, the minimum measurable quantity of BSA at 1 THz is approximately 10 picomoles (0.6 μg). Microfluidic channels offer a new platform for performing THz spectroscopy of small quantities of biomolecules using low-power THz sources.

Acknowledgments